IOP Publishing Phys. Med. Biol. 63 (2018) 05NT02 (8pp) https://doi.org/10.1088/1361-6560/aaa815

Physics in Medicine & Biology

IPEM Institute of Physics and Engineering in Medicine

NOTE

Comparison of acrylic polymer adhesive tapes and silicone optical grease in light sharing detectors for positron emission tomography

Devin J Van Elburg[1], Scott D Noble[2], Simone Hagey[2] and Andrew L Goertzen[1,3]

[1] Department of Physics and Astronomy, University of Manitoba, Winnipeg, MB R3T 2N2, Canada
[2] College of Engineering, University of Saskatchewan, Saskatoon, SK S7N 5A9, Canada
[3] Department of Radiology, University of Manitoba, Winnipeg, MB R3E 3P4, Canada

E-mail: vanelbud@myumanitoba.ca

RECEIVED
18 October 2017

REVISED
8 January 2018

ACCEPTED FOR PUBLICATION
16 January 2018

PUBLISHED
26 February 2018

Keywords: optical coupling, silicone optical grease, positron emission tomography, acrylic polymer tapes, silicon photomultiplier, photomultiplier tube, light diffuser

Abstract

Optical coupling is an important factor in detector design as it improves optical photon transmission by mitigating internal reflections at light-sharing boundaries. In this work we compare optical coupling materials, namely double-sided acrylic polymer tapes and silicone optical grease (SiG), in the context of positron emission tomography. Four double-sided tapes from 3 M of varying thicknesses (0.229 mm–1.016 mm) and adhesive materials ('100MP', 'A100', and 'GPA') were characterized with spectrophotometer measurements as well as photopeak amplitude and energy resolution measurements using lutetium-yttrium oxy-orthosilicate (LYSO) coupled to photomultiplier tubes (PMT) or silicon photomultipliers (SiPMs). Transmission spectra from the spectrophotometer showed over 80% transmission for all tapes at 420 nm and above, with 89.6% and 88.8% transmission for the 0.508 mm and 1.016 mm thick GPA tapes, respectively, at 420 nm. Measurements with single-pixel LYSO-PMT and 4 × 4 array (one-to-one coupled) LYSO-SiPM setups determined that SiG had the greatest photopeak amplitude, with tapes showing 2.1%–14.8% reduction in photopeak amplitude with respect to SiG. Energy resolution changed by less than 4% on a relative basis between tapes and SiG with PMT measurements, however for the SiPM array measurements the energy resolution improved from 15.6% ± 2.7% full-width at half-maximum to 11.4% ± 1.2% for SiG and 1 mm GPA respectively. Data acquired with dual-layer offset LYSO arrays (light sharing detector designs) demonstrated that a detector coupled with 1 mm thick GPA tape produced equivalent detector flood histograms to those from a design coupled with SiG and a 1 mm thick glass lightguide. No significant degradation in photopeak amplitude and energy resolution was observed over five months of measurements, indicating the tapes maintain their coupling integrity over several months. Though minimal photopeak amplitude degradation compared to SiG occurs, double-sided tapes are convenient alternatives for optical coupling materials since they diffuse light intrinsically, acting as a light guide, offer mechanical support and durability, are easily applied and removed from scintillators/photodetectors, and are relatively inexpensive and readily available.

1. Introduction

High quality optical coupling between scintillators, lightguides, and photosensors in scintillation detectors is necessary to maximize light collection efficiency and with it energy and timing resolution. It is well known that matching refractive index between optical boundaries will minimize internal reflections between scintillator-lightguide-photosensor boundaries. Ideally, optical coupling materials should have a refractive index that is matched to the optical boundaries they are coupling: e.g. between $n = 1.5$ and $n = 1.8$ for photodetectors and scintillators such as cerium-doped lutetium-yttrium oxy-orthosilicate (LYSO:Ce, $n = 1.82$ at 420 nm (Mao 2008)). Silicone grease (SiG) is commonly used for optical coupling (e.g. Yeom *et al* (2013), Pizzichemi *et al* (2016) and Park *et al* (2017)). Advantages of SiG include relatively good media matching ($n \approx 1.5$) and ease of

Table 1. Summary of the optical coupling materials used.

Material	3 M product #	Thickness (mm)
GPA	4910	1.016
A100	4658F	0.787
GPA	4905	0.508
100MP	F9469PC	0.229
SiG	—	~0.150[a]

[a] e.g. González *et al* (2013) modelled a layer of SiG to be 150 μm thick.

application or removal of coupling. However, SiG allows the scintillator to slide on the photodetector surface unless mechanical supports are used, slowing the setup of test detectors in a research setting and potentially permitting crystals to migrate from their original setup positions throughout data acquisition. To allow for rigid mounting, several groups have used thermally reversible adhesives such as Meltmount™ (e.g. Nemallapudi *et al* (2015), Schmall *et al* (2015), Ferri *et al* (2016), Gundacker *et al* (2016) and Morrocchi *et al* (2016)) or permanent silicone-based adhesives such as those from Dow Corning (e.g. Schneider *et al* (2015), Liu *et al* (2016) and Omidvari *et al* (2017)) for optical coupling. Epoxies or UV curing glues can also be used for rigid mounting, however these are usually non-reversible bonds.

An alternative coupling method is to use optically transparent double-sided tapes, which offer both an optical coupling medium and a means of mechanical stabilization of the detector. Tapes are easily applied without the need for curing or thermal treatments, and are easily removed if necessary. To our knowledge, a systematic comparison of the performance of tapes for optical coupling has not been done. Thus we present here a comparison of the performance of various double-sided tapes and SiG for optical coupling.

2. Materials

2.1. Optical coupling materials

Four double-sided, acrylic polymer tapes from 3 M (Saint Paul, MN) were investigated in this study. Two tapes with thickness 1.016 mm and 0.508 mm, from the 3M VHB class, were a general purpose acrylic ('GPA') adhesive on a foam carrier. One tape with 0.229 mm thickness, also in the VHB family, contained '100MP' acrylic adhesive without a carrier or backing. Lastly, one tape with 0.787 mm thickness consisted of Adhesive 100 material ('A100') deposited on an acrylic foam carrier. These tapes, summarized in table 1, were selected because of their off-the-shelf availability and their wide range of thicknesses. It should be noted that these tapes are not specifically designed for optical purposes. The SiG used for comparison was Visilox V-788 (Rhone-Poulenc Silicones VSI, Troy, NY) silicone optical compound.

3. Methods

3.1. Spectrophotometer measurements

Four samples of each tape were mounted to cardboard holders with a 12 mm by 17 mm aperture. This allowed the paper liners to be removed from the tapes without the tape sticking to the table or instrument. Samples were secured to the solid sample holder of a Cary 5G dual-beam spectrophotometer (Agilent, Santa Clara, CA) in transmission mode, with only air in the reference beam path. Transmission data were obtained over a range of 300–800 nm at 1 nm increments with a 2 nm spectral band width for each sample. The mounting stage did not allow for SiG testing without avoiding transmission through supporting media, thus SiG transmission data were not obtained.

3.2. PMT—single LYSO:Ce crystal

A single Teflon-wrapped 10 × 10 × 10 mm^3 LYSO:Ce crystal (Proteus Inc., Chagrin Falls, OH) was coupled to a Hamamatsu H3178-51 photomultiplier tube (PMT) that was mounted in a light-tight box. The PMT output was processed using conventional NIM electronics and the signal digitized using a National Instruments PCI-6133 data acquisition card controlled by software written in National Instruments LabWindows/CVI. Data were subsequently processed using software developed in MATLAB 2016a (MathWorks, Natick, MA). The photopeak of the energy spectrum of each material was fit to a Gaussian plus line function $F(x)$:

$$F(x) = Ae^{-\left(\frac{x-\mu}{\sqrt{2}\sigma}\right)^2} + mx + b \quad (1)$$

where A, μ, and σ are the amplitude, centre, and standard deviation, respectively, of the Gaussian; m and b are the slope and intercept, respectively, of the line; and x is the ADC value in volts. From these fit parameters, the 511 keV photopeak amplitude and the full-width at half-maximum (FWHM) energy resolution are obtained as:

$$\text{Photopeak ampitude} = \mu \tag{2}$$

$$\text{Energy resolution} = \frac{2.355\sigma}{\mu} \times 100\%. \tag{3}$$

For each optical coupling material, 10^6 counts were acquired using a ^{68}Ge rod source with activity ~2.5 MBq.

3.3. SiPM array—single-layer 4 × 4 LYSO:Ce array

Use of double-sided tapes with array detectors was evaluated using an 8 × 4 silicon photomultiplier (SiPM) array assembled using two SensL MicroFC-30035-16P-PCB arrays (SensL, Cork, Ireland). These arrays use the 3 × 3 mm^2 C-series SiPM assembled on a 4.2 mm pitch. For all measurements the arrays were biased at 29.0 V. The SiPM outputs were multiplexed using a charge division resistor network to reduce the number of signals from 32 to four, similar in design to those previously reported by Liu and Goertzen (2014). The SiPM/PCB apparatus was placed in a thermally insulated light-tight box. Similar to the PMT setup, the multiplexed SiPM signals were processed using conventional NIM shaping amplifier electronics and digitized with the National Instruments PCI-6133 card (as previously described by Goertzen *et al* (2013)). An in-house developed MATLAB based software package was used to generate detector flood images using simple Anger-type logic, to segment the flood image into individual crystal regions, and to calculate the photopeak amplitude and energy resolution on a per-crystal basis. No saturation correction was applied to the energy spectra since a linearity correction is expected to have minimal impact on the measured energy resolution, based on previous work by Thiessen *et al* (2013) showing approximately a 1% absolute change in energy resolution following linearity correction with a similar detector design.

A 4 × 4 array of 4 × 4 × 4 mm^3 LYSO:Ce crystals (Midas Applied Materials Corp., Zhubei City, Taiwan) was constructed in-house with 3 M enhanced specular reflector (ESR) outer-wrapping and air gaps between crystals. This array was directly coupled (i.e. without any intermediary light diffuser) to one of the 4 × 4 SiPM arrays, providing approximately one-to-one coupling between scintillator and SiPM pixels (albeit with light sharing between crystals). For each optical coupling material, 1.14 × 10^6 counts were acquired using a ^{22}Na point source (~1.8 MBq) embedded in an acrylic 10 × 10 × 10 mm^3 cube. Photopeak amplitude and energy resolution results were averaged and standard deviations calculated across the 16 crystals in the array for each coupling case.

3.4. SiPM array—9 × 9/8 × 8 DLO LYSO:Ce array

The same SiPM detector and readout was used as described in section 3.3. A dual-layer offset (DLO) LYSO:Ce array (Proteus Inc., Chagrin Falls, OH), with a 9 × 9 bottom layer array of 1.41 × 1.41 × 6 mm^3 crystals and a half crystal pitch offset 8 × 8 top array of 1.41 × 1.41 × 4 mm^3 crystals, was coupled to the 4 × 4 section of the SiPM array. The LYSO:Ce array was coupled to the SiPM array on the 9 × 9 bottom layer. Since the DLO array crystal density is greater than the SiPM pixel density for this light-sharing detector setup, a light diffuser must be coupled between the scintillator and SiPMs to ensure sufficient light spread for identification of individual crystals in the detector flood image. Hence for these measurements the DLO array was coupled with SiG to a 0.96 mm thick glass lightguide for all coupling cases, then the bottom side of the lightguide was coupled with either SiG or the adhesive tapes to the SiPM array. For each coupling condition, 5 × 10^6 counts were obtained with the ^{68}Ge rod source. Upon qualitative assessment of crystal resolvability of the detector flood images, it was clear that the use of lightguides as diffusers for the thickest tapes was unnecessary. Consequently, additional data were obtained for the case of coupling the scintillator array using 1.016 mm GPA without the lightguide.

3.5. SiPM array—26 × 13/25 × 12 DLO-LYSO:Ce array with ESR grid

The same SiPM apparatus and readout was used as described in section 3.3. A DLO LYSO:Ce array (Proteus Inc., Chagrin Falls, OH), with a 26 × 13 bottom layer of 1.28 × 1.28 × 6 mm^3 crystals and a half crystal pitch offset 25 × 12 top layer of 1.28 × 1.28 × 4 mm^3 crystals, was coupled to the 8 × 4 SiPM array. The 26 × 13 bottom LYSO:Ce layer was coupled to the SiPM array. A custom ESR grid was attached to the SiPM array, covering the dead space between pixel sensitive regions, to enhance light collection. A light-collection-optimized lightguide was constructed with this ESR grid on the SiPM-coupling face, ESR on the outer faces, and no wrapping on the scintillator-coupling face (Agile Technologies, Knoxville, TN). When using tape, the ESR grid was first placed onto the SiPM array, then 1 mm GPA tape was applied overtop. Four acquisitions of 10^7 counts each were obtained with the ^{68}Ge rod source under coupling conditions of: (i) 1 mm GPA tape only, (ii) 1 mm GPA tape and the ESR grid, (iii) SiG and a 0.96 mm lightguide, and (iv) SiG and a 0.96 mm lightguide with the ESR grid.

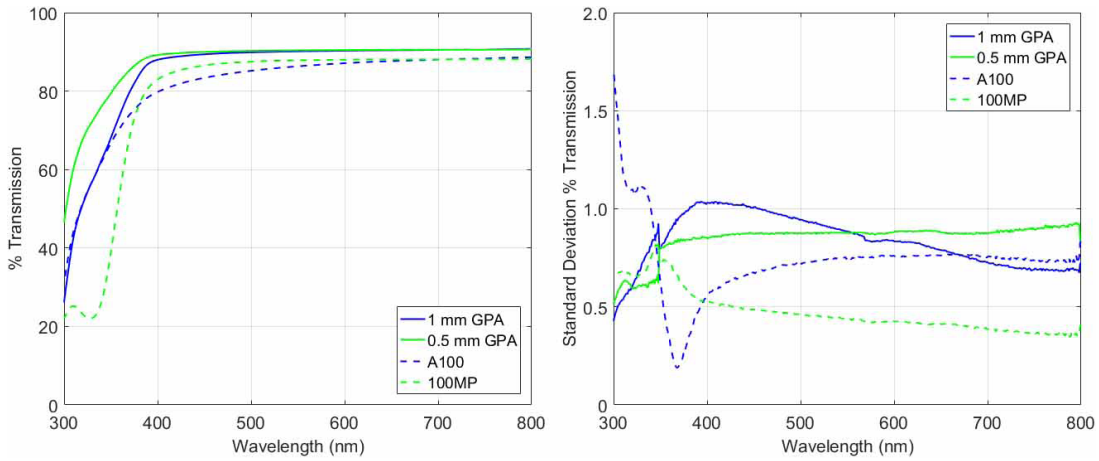

Figure 1. Average transmission (left) and standard deviation (right) between four samples of each tape.

Table 2. Photopeak amplitude and energy resolution of the 511 keV photopeak for the Teflon-wrapped $1 \times 1 \times 1\,cm^3$ LYSO:Ce crystal coupled to the Hamamatsu type PMT.

Material	Thickness (mm)	Photopeak (V)	Energy resolution (%)
GPA	1.016	1.36	10.9
A100	0.787	1.30	11.0
GPA	0.508	1.36	10.9
100MP	0.229	1.31	11.2
SiG	—	1.44	10.8

3.6. Tape stability over time

To observe the integrity of the tapes over time, the PMT (section 3.2) and SiPM-DLO (section 3.4) detectors, coupled with 1 mm GPA tape, were left untouched for over five months. During this time, repeated measurements were taken of photopeak amplitude and energy resolution. The only difference in setup was that the SiPM-DLO detector was placed in a temperature regulating box which was maintained at 20.0 °C. With the ^{68}Ge rod source, 2×10^6 and 5×10^6 counts were obtained with the PMT and SiPM, respectively. Energy spectra were produced for the PMT and all SiPM pixels. For the $9 \times 9/8 \times 8$ DLO array, pixel-by-pixel averaged energy resolution for the central 5×5 bottom-layer-pixels and central 4×4 top-layer-pixels were obtained.

4. Results

4.1. Spectrophotometer measurements

The left plot of figure 1 shows the transmission spectra averaged over the four samples of each tape. At 420 nm, the GPA tapes had the greatest transmission at 89.6% and 88.8% for 0.5 mm and 1.0 mm thicknesses, respectively, while the 100MP and A100 tapes showed 85.1% and 81.6% transmission, respectively. Note that these transmission spectra demonstrate optical transmission between air-tape-air interfaces rather than detector geometries with scintillator-tape-photodetector interfaces. The right plot in figure 1 demonstrates the reproducibility between samples, as the standard deviation between the four samples was near or below 1% for wavelengths above 400 nm for all tapes.

4.2. PMT—single LYSO:Ce crystal

PMT measurements results are summarized in table 2. The largest photopeak amplitude was measured with SiG. Consistent with the 420 nm transmission data obtained in section 4.1, the GPA tapes resulted in greater photopeak amplitude than 100MP and A100. Photopeak amplitude reduction of the tapes compared to SiG ranged from 5.6% to 9.5%. Energy resolution of the tapes showed marginal degradation of about 3.7% relative to SiG, with an absolute range of energy resolution of 10.8% (SiG) to 11.2% (100MP).

4.3. SiPM array—single-layer 4×4 LYSO:Ce array

Results from the one-to-one coupling of the LYSO:Ce array to SiPM array are summarized in table 3. Similar to the PMT results, the largest photopeak amplitude was measured with SiG at (5.82 ± 0.17) V. The tapes gave a photopeak degradation range between 2.1% (0.5 mm GPA) and 14.8% (100MP).

Table 3. Pixel-by-pixel averaged photopeak amplitude and energy resolution of the 511 keV photopeak for the 4 × 4 LYSO:Ce crystal array coupled to the 4 × 4 SensL SiPM array.

Material	Thickness (mm)	Photopeak (V)	Energy resolution (%)
GPA	1.016	5.36 ± 0.17	11.4 ± 1.2
A100	0.787	5.41 ± 0.18	12.3 ± 1.4
GPA	0.508	5.70 ± 0.16	11.7 ± 1.3
100MP	0.229	4.96 ± 0.34	14.0 ± 1.5
SiG	—	5.82 ± 0.25	15.6 ± 2.7

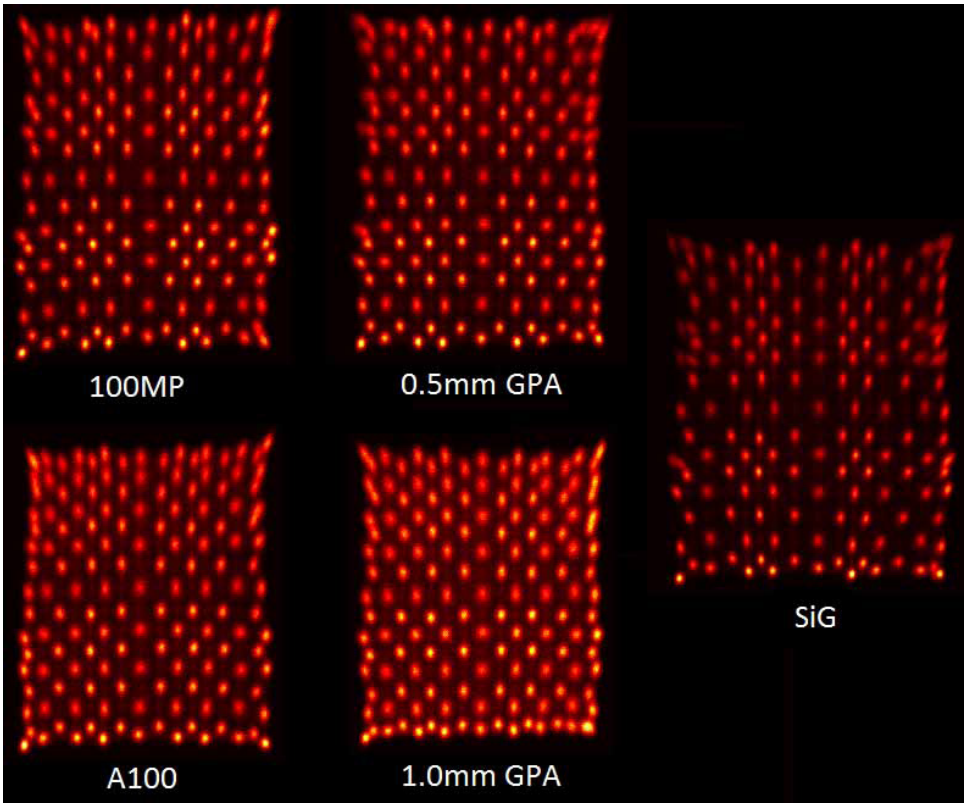

Figure 2. 9 × 9/8 × 8 DLO array flood maps. The DLO array is coupled to a 0.96 mm lightguide with SiG, then coupled to the SiPM array with 100MP, 0.5 mm GPA, A100, 1.0 mm GPA, or SiG.

Energy resolution was poorest for SiG at (15.6 ± 2.7)% and best for the 1.016 mm GPA at (11.4 ± 1.2)%. We believe the reason for improvement of energy resolution with tapes may be explained by light diffusion. This 4 × 4 array setup is not truly one-to-one coupling; the pitch of the scintillator pixels is 4.0 mm while the pitch of the SiPM pixels is 4.2 mm. Loss of energy resolution may be a result of imperfect crystal alignment and inter-crystal light sharing. However the effect of scintillator misalignment is minimized as the diffusion layer thickness (i.e. tape thickness) increases, since the optical photons penetrating the tapes are distributed over a larger area of the SiPMs, leading to more uniform collection of light from each crystal. Assuming SiG is the thinnest coupling material (for example, González *et al* (2013) modelled a layer of SiG ~150 μm thick), then it is expected that the energy resolution is poorer for SiG and should improve with thicker tapes.

4.4. SiPM array—9 × 9/8 × 8 DLO-LYSO:Ce array

The importance of light diffusion is evident when comparing flood maps of the DLO LYSO:Ce array. Crystals are well resolved in flood maps of all coupling materials, however there are differences in the appearance of the flood histograms (see figure 2). The crystal 'dot' size gets noticeably larger for thicker tapes, suggesting a decreasing peak-to-valley ratio. These effects are due to an increased diffusion layer thickness, where the SiG coupling thickness is ~1 mm with the lightguide while the 1 mm GPA coupling thickness is ~2 mm with the lightguide. As diffusion layer thickness increases, the flood maps become more condensed and the crystal dot sizes increase.

The results suggest that thick tapes may not need to be accompanied with lightguides for light sharing detectors. When using 1 mm GPA without a lightguide (figure 3, right), the flood map is nearly indistinguishable from the flood map obtained using SiG and the lightguide (figure 3, centre). For the central 5 × 5/4 × 4 crystals, the

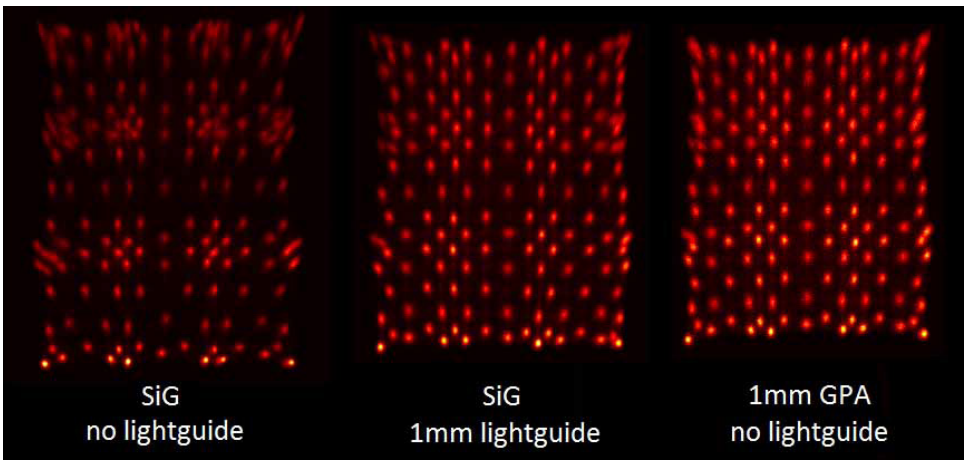

Figure 3. GPA tape versus SiG, with and without the use of a lightguide. The centre and right floodmaps were both obtained with approximately 1 mm diffuser thicknesses and are thus nearly indistinguishable. The left floodmap demonstrates the need for a diffuser in light sharing detector designs using pixelated photosensors.

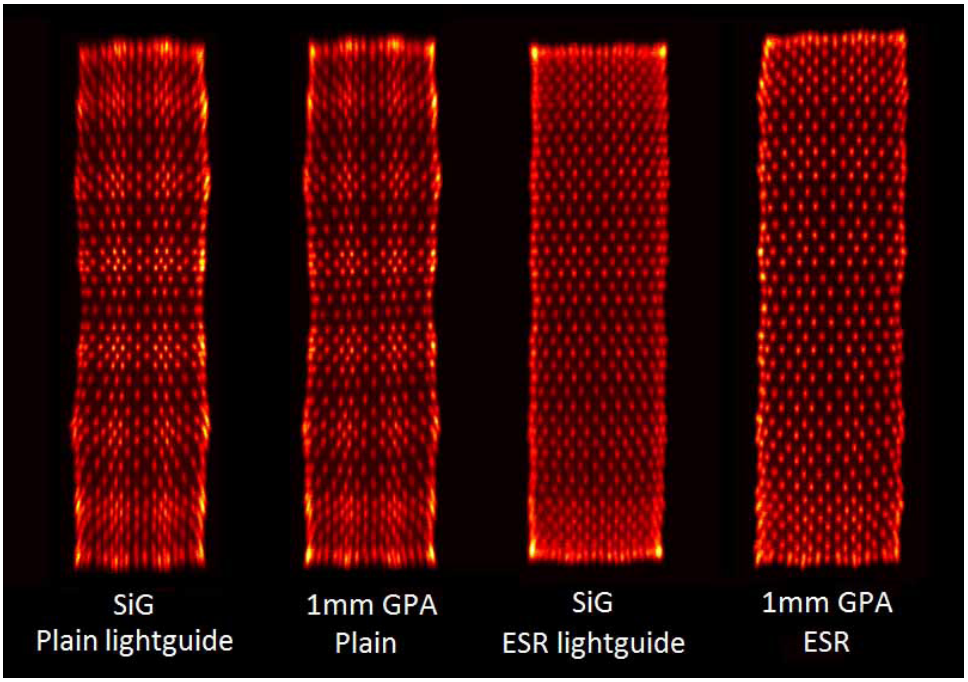

Figure 4. Demonstration of the use of tape as lightguides in light sharing detector designs.

average photopeak amplitude for the SiG-lightguide and 1 mm GPA-no-lightguide cases was (6.2 ± 0.2) V and (6.3 ± 0.2) V respectively, while the average energy resolution was (11.4 ± 1.2)% and (11.3 ± 0.9)% respectively. Here, no quantitative or qualitative difference was observed between SiG and GPA when the diffusion layers are the same thickness.

Tape as the sole diffuser has the advantage of simplicity. With the presence of a lightguide there are four medium interfaces that optical photons must traverse: scintillator-coupling, coupling-lightguide, lightguide-coupling, and coupling-photodetector. However, without a lightguide there are only the scintillator-coupling and coupling-photodetector interfaces. Since each medium interface presents opportunities for air pockets and/or optical photon internal reflection, it is ideal to keep the number of media interfaces to a minimum.

4.5. SiPM array—26 × 13/25 × 12 DLO-LYSO:Ce array with ESR grid

Figure 4 demonstrates the effect an ESR grid placed over the SiPM dead spaces has on crystal resolvability. Crystal uniformity improves across the entire flood map, and more importantly crystals are better resolved at the edges. The SiG-ESR-lightguide flood map shows better crystal resolution at the edges, while the GPA-ESR flood map better crystal separation.

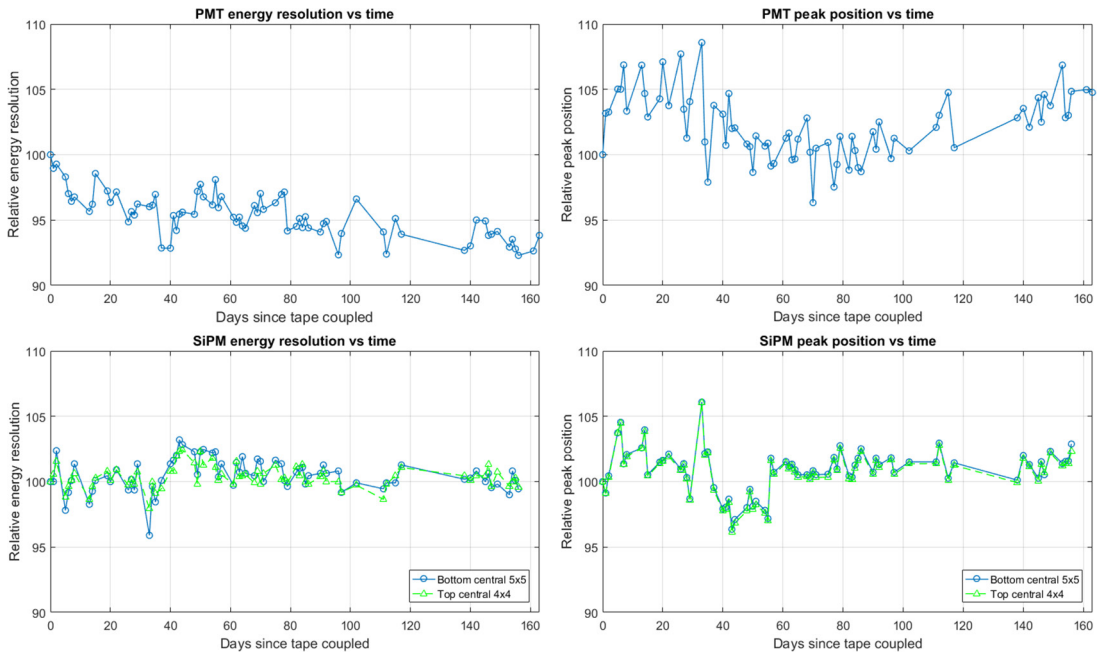

Figure 5. Plots showing stability of energy resolution (left) and peak position (right) versus time for the tape-coupled PMT (top) and SiPM (bottom) setups. The *Y*-axis is scaled relative to the Day 0 value (i.e. the ratio of a given value to the Day 0 value), which is set equal to 100. For energy resolution: 100 = 14.0%, 10.9%, and 11.0% for the PMT, SiPM bottom layer, and SiPM top layer respectively. For peak position: 100 = 437 mV, 6.08 V, and 6.73 V for the PMT, SiPM bottom layer, and SiPM top layer respectively.

One drawback to using tapes with the ESR grid is the inability of tape to flow like SiG. When applying tape to the ESR grid, air pockets between the tape-ESR-SiPM coupling were clearly visible due to the finite thickness of the ESR. Additionally, the edges of the tape-ESR flood histogram are non-uniform due to the non-rigid nature of tapes. Flood maps were expected to be better at the edges for the SiG-ESR-lightguide case since it was carefully constructed with ESR wrapping and the ESR grid by the manufacturer, while the tape was simply cut by hand and placed over the ESR grid. Using a glass lightguide and SiG has two advantages over tapes: air pockets can be eliminated due to fluid grease, and the lightguide is rigid and non-deformable.

4.6. Tape stability over time

Figure 5 shows the relative energy resolution and peak position versus time for the PMT and SiPM-DLO setups. Gradual improvement in energy resolution is seen with the PMT measurements. According to the 3 M datasheets, the GPA bond strength increases over the first few days, which could increase the quality of the coupling and hence improve energy resolution and light collection. Since PMT measurements were not temperature regulated, they were subject to the ambient temperatures in the laboratory. For example, issues with the lab room thermostat caused the room temperature to be higher and inconsistent (~21–23 °C); this issue was fixed on day 37 and the room was maintained at 20.0 °C thereafter. Consequently, PMT peak position was higher and day-to-day peak positions varied more before day 37 compared to after day 37.

The SiPM measurements show good consistency over time in the temperature regulated box. Over the 156 elapsed days, an absolute variation in energy resolution of ~0.5% was observed. The SiPM peak position generally stayed between a factor of 1.00–1.05 with respect to Day 0 (6.8–7 V), however for unclear reasons there appears to be a systematic shift to ~6.6 V for days 37–54.

5. Discussion and conclusion

Optical coupling is used to mitigate internal reflections at boundaries and allow for optimal transmission of optical photons to the photodetector. In this study, transmission spectra and photopeak amplitude measurements were performed to evaluate the optical transparency of double-sided tapes. Spectrophotometer measurements indicate greater than 80% transmission for wavelengths of greater than 420 nm for all tapes tested, with 89.6% and 88.8% transmission at 420 nm for the 0.5 mm and 1 mm GPA tapes, respectively. Due to the setup of the sample trays with the spectrophotometer, measurements also comparing SiG could not be done without complicating the measurements with additional media. However, photopeak amplitude measurements with the PMT (section 4.2) and SiPM (section 4.3) setups allow for a direct comparison between the tapes and SiG. SiG always gave the greatest photopeak amplitude, while the best performing tapes were the GPA type, with a

photopeak reduction relative to SiG of 2.1%–7.8% for the PMT and SiPM measurements. Photopeak amplitude reduction with tapes may be due to the presence of air pockets at the coupling interface. SiG has the advantage of being fluid, thus air pockets can be removed with relative ease. Malleable but non-liquid tapes make air pocket removal difficult. Air pockets introduce poorly-matched boundaries and increase light losses due to internal reflection.

In research applications where combinations of scintillators and photodetectors are constantly changing, minimal light collection degradation is acceptable for the added convenience, time savings, and avoiding need for mechanical support structures when using tapes over SiG or other coupling materials. Where more permanent coupling is required, the tapes were shown to maintain their optical coupling integrity, at least in the case of GPA, over a five month span (section 4.6).

Tape thickness is an additional advantage for light sharing designs that require diffusors. Where coupling media such as greases and glues require lightguides, thick tapes may be used as intrinsic diffusors, and therefore can simplify detector designs and decrease the number of material interfaces that cause some internal reflection and light loss. Figures 4 and 5 demonstrate how the 1 mm GPA tape diffuses light in the same way as lightguides when using SiG.

Despite small photopeak amplitude degradation compared to SiG, double-sided tapes offer a convenient alternative to conventional optical coupling media since they are readily available, are easily applied and removed, are mechanically stable, and are able to diffuse light effectively for light sharing photodetector designs.

Acknowledgments

This work was supported by the Natural Sciences and Engineering Research Council of Canada (NSERC) through Discovery Grant 341628 to AL Goertzen and through a Research Manitoba Graduate Studentship award and Manitoba Graduate Scholarship to D Van Elburg. AL Goertzen wishes to acknowledge and thank our collaborator and friend Christopher J Thompson, a longtime faculty member of the Montreal Neurological Institute, who recently passed away. We will miss his enthusiasm, his scientific insights and his constant search for simple solutions to vexing problems.

References

Ferri A, Acerbi F, Gola A, Paternoster G, Piemonte C and Zorzi N 2016 Performance of FBK low-afterpulse NUV silicon photomultipliers for PET application *J. Instrum.* **11** P03023

Goertzen A L *et al* 2013 Design and performance of a resistor multiplexing readout circuit for a SiPM detector *IEEE Trans. Nucl. Sci.* **60** 1541–9

González A J *et al* 2013 Monolithic crystals for PET devices: optical coupling optimization *Nucl. Instrum. Methods Phys. Res.* A **731** 288–94

Gundacker S, Auffray E, Pauwels K and Lecoq P 2016 Measurement of intrinsic rise times for various L(Y)SO and LuAG scintillators with a general study of prompt photons to achieve 10 ps in TOF-PET *Phys. Med. Biol.* **61** 2802–37

Liu C Y and Goertzen A L 2014 Multiplexing approaches for a 12 × 4 array of silicon photomultipliers *IEEE Trans. Nucl. Sci.* **61** 35–43

Liu Z, Pizzichemi M, Auffray E, Lecoq P and Paganoni M 2016 Performance study of Philips digital silicon photomultiplier coupled to scintillating crystals *J. Instrum.* **11** P01017

Mao R, Zhang L and Zhu R-Y 2008 Optical and scintillation properties of inorganic scintillators in high energy physics *IEEE Trans. Nucl. Sci.* **55** 2425–31

Morrocchi M, Hunter W C J, Del Guerra A, Lewellen T K, Kinahan P E, MacDonald L R, Bisogni M G and Miyaoka R S 2016 Evaluation of event position reconstruction in monolithic crystals that are optically coupled *Phys. Med. Biol.* **61** 8298–320

Nemallapudi M V, Gundacker S, Lecoq P, Auffray E, Ferri A, Gola A and Piemonte C 2015 Sub-100 ps coincidence time resolution for positron emission tomography with LSO:Ce codoped with Ca *Phys. Med. Biol.* **60** 4635–49

Omidvari N, Sharma R, Ganka T R, Schneider F R, Paul S and Ziegler S I 2017 Characterization of 1.2 × 1.2 mm^2 silicon photomultipliers with Ce:LYSO, Ce:GAGG, and Pr:LuAG scintillation crystals as detector modules for positron emission tomography *J. Instrum.* **12** P04012

Park H, Ko G B and Lee J S 2017 Hybrid charge division multiplexing method for silicon photomultiplier based PET detectors *Phys. Med. Biol.* **62** 4390–405

Pizzichemi M, Stringhini G, Niknejad T, Liu Z, Lecoq P, Tavernier S, Varela J, Paganoni M and Auffray E 2016 A new method for depth of interaction determination in PET detectors *Phys. Med. Biol.* **61** 4679–98

Schmall J P, Surti S and Karp J S 2015 Characterization of stacked-crystal PET detector designs for measurement of both TOF and DOI *Phys. Med. Biol.* **60** 3549–65

Schneider F R, Shimazoe K, Somlai-Schweiger I and Ziegler S I 2015 A PET detector prototype based on digital SiPMs and GAGG scintillators *Phys. Med. Biol.* **60** 1667–79

Thiessen J D, Jackson C, O'Neill K, Bishop D, Kozlowski P, Retière F, Shams E, Stortz G, Thompson C J and Goertzen A L 2013 Performance evaluation of SensL SiPM arrays for high-resolution PET *IEEE Nuclear Science Symp. Conf. Record* pp 1–4

Yeom J Y, Vinke R and Levin C S 2013 Optimizing timing performance of silicon photomultiplier-based scintillation detectors *Phys. Med. Biol.* **58** 1207–20